

# Deep Learning Technique for MRI-Based Brain Tumor Classification

Zicheng Zhang

Department of Arts and Science, New York University, New York, United States

zz3659@nyu.edu

**Abstract.** Brain tumors represent a severe threat to human health due to their potential to disrupt vital functions controlled by the brain, such as movement, sensation, and cognition. This study aims to classify a comprehensive dataset of 7,023 magnetic resonance imaging (MRI) images from Figshare, SARTAJ, and BR35H into four distinct classes (Glioma, Meningioma, Pituitary, and No-Tumor). After evaluating the state-of-the-art models including VGG16, DenseNet201, ResNet50, and V3 Inception, the study proposes a novel Convolutional Neural Network (CNN) model with multiple inception layers. As a result, the model achieved an accuracy of 98.71% and high AUC scores for all four categories. These results suggest the potential of this model in enhancing diagnostic accuracy and reducing radiologist workload in clinical applications. Further improvements could focus on advanced feature extraction and integration of multi-parametric MRI data. The model's robustness and effectiveness underscore its potential utility in real-world clinical settings for accurate tumor classification.

**Keywords:** Brain Tumor, Convolutional Neural Network, MRI scan, Deep Learning.

## 1. Introduction

The brain serves as the central command center of the human body, orchestrating a wide range of vital functions, including movements, sensation, thought, and emotion. It controls everything from the simplest reflexes to complex cognitive processes, ensuring the body operates harmoniously. Given its critical role, any abnormalities in the brain can have profound implications. Statistically, brain tumors also prove a significant concern. With approximately 25,400 new diagnoses and an estimated 18,760 deaths expected in the United States in 2024 alone [1]. Malignant brain tumors, which are more aggressive, have a particularly high mortality rate, with the five-year survival rate being around 33.4% for malignant cases [2]. This highlights the urgent need for effective diagnostic and treatment strategies.

Magnetic Resonance Imaging (MRI) is extensively used to detect brain tumors due to its superior ability to differentiate soft tissues. MRI provides detailed images of the brain, allowing for accurate tumor localization and characterization without exposing patients to ionizing radiation. However, relying solely on MRI has several drawbacks. MRI images can suffer from noise and artifacts, which may obscure critical details. The process is also time-consuming and requires significant expertise to interpret accurately. Additionally, MRI scans may not always provide sufficient information about the tumor's metabolic activity or genetic profile, which are crucial for personalized treatment planning [3].

To address these limitations, recent advancements in medical imaging have integrated MRI with other technologies and employed advanced methods such as Deep Learning (DL) for improved tumor detection and classification. Many techniques, ranging from Artificial Neural Networks (ANN), Convolutional Neural Networks (CNNs), and Support Vector Machines (SVM) have shown great promise in automating the analysis of MRI images, enhancing diagnostic accuracy, and reducing the workload on radiologists. These models can learn significant features from extensive datasets, making them particularly adept at differentiating between various brain tumor types and evaluating their severity.

This study aims to design and assess a convolutional neural network (CNN) model to classify brain tumors using MRI images. The research methodology includes data preprocessing, feature extraction, model training, and evaluation. The convolutional neural network (CNN) model selected contributed to its significant advantages in handling image data, including automatic extraction of high- and low-level features, strong spatial invariance, and excellent performance in various image classification tasks. CNNs effectively capture local features in images and build complex representations by stacking multiple convolutional layers, making them highly suitable for medical image analysis, making it effective for disease detection in medical domains.

However, despite the outstanding performance of CNNs in many applications, there are still some challenges. CNN models typically necessitate a substantial amount of labeled data for effective training, which can be challenging to collect in the medical field. To address these issues, this paper combines a dataset from three distinct authoritative medical sources and applies enhanced preprocessing aiming to enhance the model's classification performance.

## **2. Method**

### **2.1. Dataset**

The dataset of this project is a comprehensive compilation derived from the Figshare, SARTAJ, and Br35H datasets. It encompasses T1-weighted, T2-weighted, and FLAIR MRI images, amounting to a total of 7,023 human brain MRI scans with confirmed diagnoses. MRI (Magnetic Resonance Imaging) is preferred over CT (Computed Tomography) scans since MRI offers superior soft tissue contrast, providing exceptional differentiation between various types of soft tissues. This allows for more detailed and clearer images of the brain's structures, making it easier to distinguish between normal and abnormal tissues. This high contrast is particularly beneficial for identifying brain tumors, as it helps in precisely locating the tumor and assessing its boundaries [4]. The datasets are categorized into four distinct and balanced labels/classes: no tumor (2,000 images), glioma (1,621 images), meningioma (1,645 images), and pituitary tumor (1,757 images). Each category includes images captured from axial, coronal, and sagittal view planes. For model training and validation, 80% of the images were allocated to train the Convolutional Neural Network (CNN) model, while the remaining 20% were reserved for testing.

### **2.2. Preprocessing**

The preprocessing of MRI images in this study involves several critical steps to ensure that the data is suitable for training and evaluating our deep learning models. These steps include labeling, image cropping, normalizing and resizing, noise filtering, edge detection using the Canny method, data augmentation, and feature extraction.

**Labeling:** Initially, all MRI images are labeled according to their respective categories. The dataset is categorized into four distinct labels: no tumor, glioma, meningioma, and pituitary tumor. Accurate labeling is essential as it serves as the foundation for supervised learning, allowing the model to learn the features specific to each class.

**Image Cropping:** Following labeling, the images are cropped to eliminate the margins of images and focus on areas of brain tumors. This is particularly essential because the datasets contain images of different sizes. Cropping to remove extra margins helps in removing irrelevant background information that could potentially interfere with the learning process. By focusing on the relevant region, the model can learn more efficiently and effectively.

**Normalization and Resizing:** Since the images could be taken under different protocols, scanners, and conditions, the intensities of the images may not be consistent [5]. Additionally, MRI images can vary in terms of resolution, contrast, and presence of artifacts. Therefore, Min-Max normalization is employed to adjust the pixel intensity values to a standard range, typically between 0 and 1, which helps in improving the convergence of the neural network during training [6, 7]. Additionally, resizing

is done to ensure that all images have a uniform dimension – 128x128, ensuring compatibility with the input requirements of the CNN architecture used.

**Noise Filtering:** Noise in MRI images can significantly affect the performance of image classification. Therefore, noise filtering techniques are applied to improve the quality of the images. Gaussian filtering, in particular, is utilized to reduce noise and smooth the images in this study.

$$G(x, y) = \frac{1}{\sqrt{2\pi}\sigma^2} e^{-\frac{x^2+y^2}{2\sigma^2}} \quad (1)$$

The processed MRI images enhance image quality by averaging out random variations while preserving important features. This filter, characterized by its non-uniform kernel where central pixels have higher weights, effectively reduces noise but can also result in a slight loss of image brightness [8]. Overall, this method makes it easier for the model to detect and classify brain tumors accurately.

**Canny Edge Detection:** To further enhance the image quality and highlight important features, a CV based - Canny edge detection algorithm was applied. This method helps in identifying the edges within the images, which are critical for distinguishing different structures and features of the brain. Edge detection aids in emphasizing the boundaries of the tumors, making it easier for the model to learn these distinctions.

**Data Augmentation:** Augmentation is essential for CNN-based architecture to avoid overfitting. As a result, this study artificially increases the diversity and size of the training dataset. This method includes rotations, translations, flips, and zooms of the input training datasets. With this geometric transformation, five times the original number of training datasets are generated randomly for training the model. These transformations help in making the model robust to variations and improve its generalization capability [9].

### 2.3. Classification

The paper uses a newly designed CNN architecture that contains few inception layers after VGG16, ResNet-50, DenseNet201 and V3 inception model are evaluated. V3 Inception model is found the most effective and therefore, the new architecture is modified based on an architecture first proposed by Soheila Saeedi and the inception module structure in the V3 Inception model, shown in Fig. 1 [10].

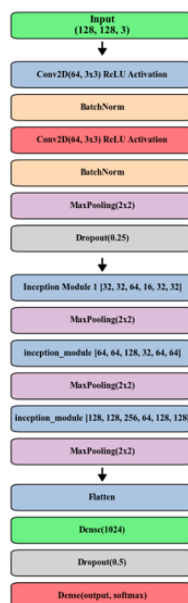


**Fig.1** The structure of the CNN (Photo/Picture credit: Original).

### **2.3.1. Convolutional Layers**

The model begins with two convolutional layers, each with 64 filters and a kernel size of 3x3. These layers use ReLU activation to introduce non-linearity. Convolutional layers are essential for learning spatial hierarchies in images, capturing local patterns like edges and textures. Additionally, batch normalization is applied after each convolutional layer to normalize the input to the subsequent layer, thereby stabilizing and accelerating the training process [11].

### **2.3.2. Max Pooling Layers**

After each set of convolutional and batch normalization layers, a max pooling layer with a pool size of 2x2 is applied. Max pooling reduces the spatial dimensions of the feature maps, which decreases the number of parameters and computations in the network. This helps to make the model invariant to small translations in the input [12].

### **2.3.3. Dropout Layers**

Dropout layers are incorporated with a dropout rate of 0.25 initially and 0.5 later in the network. This is a regularization method that helps in preventing overfitting and improves generalizability by randomly deactivating a portion of input units during training. This ensures and prevents from dependency between units and therefore forces the network to learn more generalized and robust features, to prevent extreme overfitting prone to deep networks. [13].

### **2.3.4. Inception Modules**

The model incorporates three Inception modules, which are a key component designed to capture multi-scale features. Each Inception module performs convolutions with multiple filter sizes (1x1, 3x3, 5x5) and a max pooling operation in parallel, concatenating their outputs. This architecture allows the model to capture features at various scales and levels of abstraction, enhancing its ability to recognize complex patterns in the data.

Inception Module 1: This module combines filters of sizes [32, 32, 64, 16, 32, 32], which capture different levels of detail. The inclusion of 1x1 convolutions helps reduce the dimensionality before the larger convolutions, reducing computational cost.

Inception Module 2: This module builds on the first with larger filter sizes [64, 64, 128, 32, 64, 64]. The increased filter sizes and numbers capture more complex and abstract features, improving the model to differentiate between subtle differences in tumor types.

Inception Module 3: The final Inception module uses even larger filters [128, 128, 256, 64, 128, 128], allowing the model to capture very high-level features and global information in the images. This module is critical for recognizing complex and large-scale patterns that might be indicative of different tumor classes.

Each Inception module is followed by a max pooling layer to further reduce spatial dimensions and computational load. This Inception architecture, originally proposed in the GoogLeNet model, has been shown to significantly enhance the representational power of CNNs [14].

### **2.3.5. Fully Connected Layers and Dropout**

The fully connected layer consists of 1024 neurons with ReLU activation. This layer is crucial for combining the features extracted by the convolutional and Inception modules into a form suitable for classification. It aggregates the information to make final predictions [15].

### 3. Result

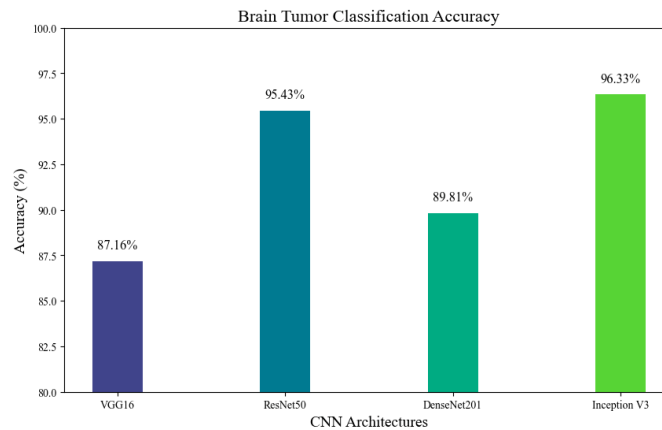


**Fig. 2** Accuracy Comparison (Photo/Picture credit: Original).

The dataset is evaluated on the four state-of-the-art structures with the accuracy rate showcased in Fig. 2. Given the figure, VGG16 achieves the minimum accuracy while Inception V3 gives the highest accuracy for classifying brain tumors.

Comparing the model structures, VGG16 is a sequential model with 16 weight layers. Its simplicity and ease of implementation are strengths, but it has limited depth and feature extraction capabilities, resulting in lower accuracy. Moreover, it results in a comparably long training time, making it inefficient for clinical applications. ResNet50, with its 50 layers and residual connections, prevents vanishing gradients and allows for effective training of deeper networks, leading to high accuracy. However, it comes also with higher computational cost and complexity. DenseNet201, a dense network with 201 layers, uses dense connections to improve gradient flow and feature reuse. While it is efficient and has good performance, its accuracy is slightly lower compared to ResNet50 and Inception V3.

Inception V3 stands out due to its unique structure of Inception modules, which apply multiple convolutional filters of different sizes in parallel. This enables multi-scale feature extraction, making the network highly effective in capturing diverse patterns in the tumor images.

Based on these findings, the proposed model structure is developed on the structure firstly proposed by Soheila Saeedi but incorporates key elements from the Inception architecture due to the superior performance of Inception V3 [10]. The model's structure is described in section 2.3 and Fig. 1. This design leverages the multi-scale feature extraction capability of Inception modules, allowing the model to capture diverse and complex patterns in MRI images effectively.

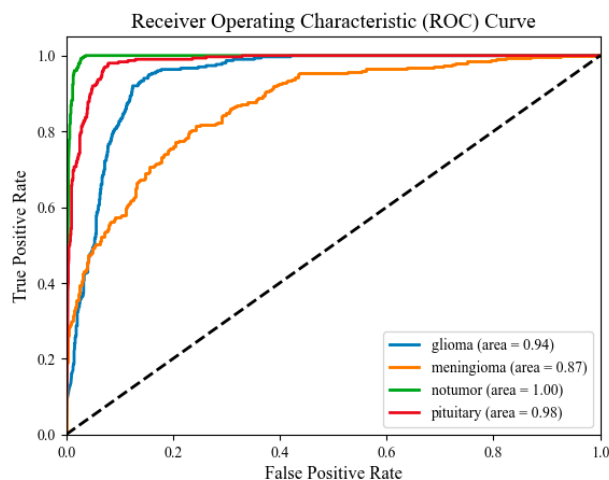


**Fig. 3** AUC scores for the proposed CNN architecture (Photo/Picture credit: Original).

The model is trained under a batch size of 32, epochs of 30, and SGD as the optimizing method, with a learning rate of 0.001. The accuracy, AUC score, and confusion matrix heatmap graph are mapped for performance evaluation. Fig. 3 provides the calculated Area Under the Curve (AUC) score for the four categories. AUC illustrates the diagnostic ability of a binary classifier system at various threshold settings which proves an efficient evaluation metric. This makes AUC robust and effective in assessing the model's discrimination ability, or its capacity to distinguish between classes. A higher AUC value indicates a better-performing model, with values closer to 1.0 denoting excellent discrimination.

The ROC curve for glioma (blue line) shows a high AUC of 0.94, 0.87 for meningioma, 1.00 for no tumor, and 0.98 for pituitary tumors. Additionally, all the curve converges sharply away from the chance line, which signifies robust performance in identifying tumor types accurately. In particular, the model performs exceptionally well in identifying no tumor and pituitary tumor cases, with nearly perfect classification reflected in the near-maximum AUC values, suggesting high sensitivity and low false positive rates across various thresholds. However, it shows limitations in distinguishing meningioma tumors, which is evident from the lower AUC and the shape of the ROC curve. Although the dataset contains slightly more nontumor images than the other, class imbalance is minor and can affect the result. Therefore, while the model performs well, there is a clear need to enhance accuracy for meningioma classification.

Overall, the high AUC values observed in the study underscore the model's effectiveness and reliability, highlighting its potential utility in clinical settings.

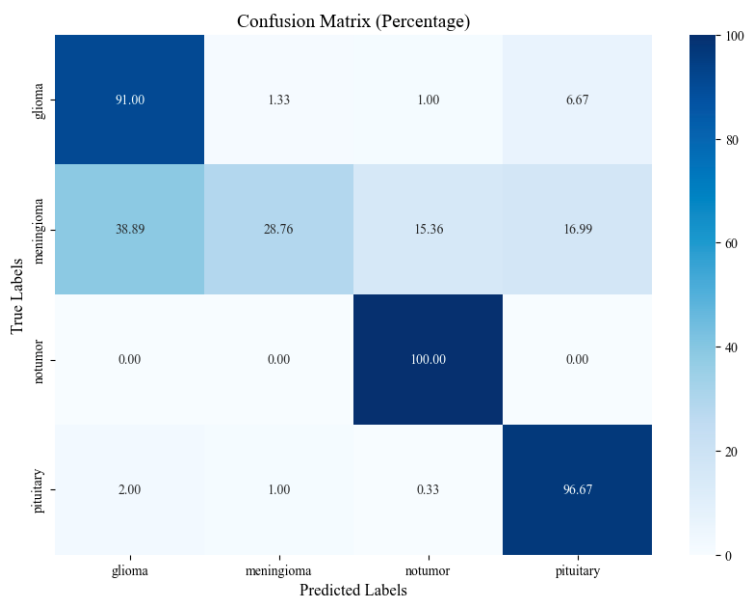


**Fig. 4** Confusion Matrix Heatmap (Photo/Picture credit: Original).

The confusion matrix provides a detailed evaluation of the brain tumor classification model's performance across four classes: glioma, meningioma, no tumor (no tumor), and pituitary tumor. Fig. 4 shows the percentage of true labels versus predicted labels for each tumor type. The model shows high accuracy in identifying glioma cases, correctly classifying 91.00% of them while misclassifying 1.33% as meningioma, 1.00% as no tumor, and 6.67% as pituitary tumors. For meningioma, the model performs less effectively, with only 28.76% correctly identified and significant misclassifications: 38.89% as glioma, 15.36% as no tumor, and 16.99% as pituitary tumors. The model perfectly identifies all no-tumor cases (100%), indicating no misclassifications in this category and nearly perfect for pituitary tumors -- strong performance with 96.67% correctly classified, and minor misclassifications: 2.00% as glioma and 1.00% as meningioma. This analysis highlights the model's strengths in identifying glioma and pituitary tumors while indicating areas for improvement in distinguishing meningioma from other classes.

## 4. Discussion

The confusion matrix reveals that the model achieves perfect accuracy in identifying the no tumor class, with 100% of no tumor instances correctly classified and no misclassifications. This high accuracy can be attributed to the distinct features present in MRI images of healthy brain tissue compared to those with tumors. Healthy brain images lack the irregularities, masses, and anomalies that are characteristic of tumor-bearing images, making them easier for the model to distinguish. The absence of these abnormal features likely provides clear, consistent patterns that the model can learn effectively. In contrast, the model struggles more with identifying specific tumor classes such as meningioma and glioma. For instance, the model only correctly identifies 16.34% of meningioma cases, with significant misclassifications into other categories like glioma (50.00%) and pituitary tumors (17.97%). These challenges can arise from several factors. One of the biggest difficulties laid upon is the similarity between gliomas and meningiomas.

Gliomas and meningiomas, two of the most common types of brain tumors, can often present similar features in imaging studies, making them challenging to differentiate. Both tumor types may appear as mass lesions with similar enhancement patterns after contrast administration on MRI, which can contribute to the misclassification observed in the confusion matrix. According to Liu, "Gliomas and meningiomas can exhibit overlapping imaging characteristics, such as irregular borders and heterogeneous enhancement, which complicate the differentiation process"[16].

**Morphological Overlap:** Gliomas and meningiomas may share similar morphological features such as irregular shapes and heterogeneous signal intensities, leading to confusion in classification. This overlap is compounded by the fact that both types of tumors can present in various locations within the brain, further complicating their differentiation.

**Heterogeneity Within Tumor Types:** Both gliomas and meningiomas exhibit a high degree of heterogeneity. Gliomas, for instance, range from low-grade to high-grade, with varying degrees of aggressiveness and imaging features. Meningiomas also display a spectrum of characteristics based on their location and histological subtype. This heterogeneity can make it challenging for the model to learn clear and distinct features for each class [17].

## 5. Conclusion

In this research, the paper has developed a convolutional neural network (CNN) model to classify brain tumors in MRI images. The focus has been on distinguishing between gliomas, meningiomas, pituitary tumors, and healthy tissues. The model demonstrated high accuracy in classifying gliomas and pituitary tumors but faced challenges in accurately identifying meningiomas due to overlapping features.

The proposed structure was trained and tested on the combination of openly accessible dataset Figshare, SARTAJ, and Br35H which achieved an accuracy of 98.71%. A large number of available images provides evidence for the model's efficiency and robustness under images taken with different circumstances and protocols.

Despite the success in certain areas, the confusion matrix revealed some challenges and spaces for improvement, particularly in identifying meningiomas. To address these issues, feature extraction with radiomics and the incorporation of multi-parametric MRI data may be incorporated beforehand.

In conclusion, while our CNN model shows promise in automating the classification of brain tumors, further refinement and enhancement can be made by incorporating CNN or auto-encoder for feature extraction, primarily focusing on the morphological similarities between tumors. Additionally, integrating hyper-tuning for generalizability will advance the model's robustness and reliability for clinical application under large datasets. This research leverages deep learning techniques to improve brain tumor diagnostics, ultimately aiming to alleviate radiologist's work and enhance accurate diagnosis through more timely interventions.

## References

- [1] Key Statistics for Brain and Spinal Cord Tumors. (n.d.). American Cancer Society. Retrieved on June 18, 2024. Retrieved from: <https://www.cancer.org/cancer/types/brain-spinal-cord-tumors-adults/about/key-statistics.html>
- [2] Cancer of the Brain and Other Nervous System - Cancer Stat Facts. (n.d.). SEER. Retrieved on June 18, 2024. Retrieved from: <https://seer.cancer.gov/statfacts/html/brain.html>
- [3] Key Statistics for Brain and Spinal Cord Tumors. (n.d.-b). American Cancer Society. Retrieved on June 18, 2024. Retrieved from: <https://www.cancer.org/cancer/types/brain-spinal-cord-tumors-adults/about/key-statistics.html>
- [4] Developer. MRI vs. CT scan. Health Images. August 30, 2021. Retrieved on June 18, 2024. Retrieved from: <https://www.healthimages.com/mri-vs-ct-scan/>
- [5] Mohan G, Subashini M M. MRI based medical image analysis: Survey on brain tumor grade classification. *Biomed. Signal Processing Control*. 2018, 39, 139-161.
- [6] Xie Y, Zaccagna F, Rundo L, et al. Convolutional neural network techniques for brain tumor classification (from 2015 to 2022): review, challenges, and future perspectives. *Diagnostics*, 2022, 12(8), 1850.
- [7] Havaei M, Davy A, Warde Farley D, et al. Brain tumor segmentation with deep neural networks. *Medical Image Analysis*, 2017, 35, 18-31.
- [8] Ravinder M, Saluja G, Allabun S, et al. Enhanced brain tumor classification using graph convolutional neural network architecture. *Scientific Reports*, 2023, 13(1).
- [9] ZainEldin H, Gamel S A, El-Kenawy E S M, et al. Brain tumor detection and classification using deep learning and sine-cosine fitness grey wolf optimization. *Bioengineering*, 2022, 10(1), 18.
- [10] Saeedi S, Rezayi S, Keshavarz H, et al. MRI-based brain tumor detection using convolutional deep learning methods and chosen machine learning techniques. *BMC Medical Informatics and Decision Making*, 2023, 23(1).
- [11] Krizhevsky A, Sutskever I, Hinton G E. ImageNet classification with deep convolutional neural networks. *Advances in Neural Information Processing Systems*, 2012, 25, 1097-1105.
- [12] Ranzato M, Boureau Y L, Chopra S, et al. Efficient learning of sparse representations with an energy-based model. *Advances in Neural Information Processing Systems*, 2017, 20, 1137-1144.
- [13] Srivastava N, Hinton G, Krizhevsky A, et al. Dropout: A simple way to prevent neural networks from overfitting. *Journal of Machine Learning Research*, 2014, 15(1), 1929-1958.
- [14] Szegedy C, Liu W, Jia Y, et al. Going deeper with convolutions. *Proceedings of the IEEE Conference on Computer Vision and Pattern Recognition*, 2015, 1-9.
- [15] Glorot X, Bengio Y. Understanding the difficulty of training deep feedforward neural networks. *Proceedings of the Thirteenth International Conference on Artificial Intelligence and Statistics*, 2010, 249-256.
- [16] Liu Y, Bai Y, Zhu X. Radiomics and its emerging role in the evaluation and management of brain tumors: A review of current applications and future perspectives. *Journal of Magnetic Resonance Imaging*, 2019 50(3), 877-890.
- [17] Komura D, Ishikawa S. Machine learning methods for histopathological image analysis. *Computational and Structural Biotechnology Journal*, 2018, 16, 34-42.